Vogel-Fulcher dependence of relaxation rates in a nematic monomer and elastomer

D. Shenoy,[1] S. Filippov,[2] F. Aliev,[2] P. Keller,[3] D. Thomsen,[1] and B. Ratna[1]

[1]*Code 6900, Naval Research Laboratory, 4555 Overlook Avenue SW, Washington, DC 20375*

[2]*Department of Physics and Materials Research Center, P.O. Box 23343, University of Puerto Rico, San Juan, PR 00931-3343, Puerto Rico*

[3]*Laboratoire Physico-Chemie Curie, CNRS UMR No. 168, Institut Curie–Section de Recherche, 11 rue Pierre et Marie Curie, 75231 Paris, Cedex 05 France*

Dielectric relaxation spectroscopy is used to study the relaxation processes in a nematic monomer and the corresponding cross-linked polymer nematic liquid crystal (elastomer). In the frequency window 10 mHz to 2 GHz the monomer liquid crystal shows a single relaxation whereas the polymer exhibits three relaxation processes, two of which are quantitatively analyzed. The temperature dependence of relaxation times in both the monomer and polymer follows a Vogel-Fulcher behavior. The relaxation processes are identified with specific molecular motions and activation energies are calculated in a linear approximation for comparison with literature data.

PACS number(s): 61.30.−v, 36.20.−r, 64.70.Md, 77.22.Gm

I. INTRODUCTION

Broadband dielectric spectroscopy (BDS) in the frequency range 1 mHz–1 GHz is a powerful technique for investigations of dielectric properties of condensed matter. Application of this method makes it possible to obtain a large amount of information about different aspects of the dynamic behavior of a variety of systems. Dynamics of different physical origin such as dynamics due to molecular reorientation, dynamics of collective or surface polarization modes, as well as dynamics due to conductivity can be investigated and detailed qualitative and quantitative information characterizing these modes can be obtained.

In particular, BDS is a powerful tool for understanding molecular relaxation processes in liquid crystals (LCs) [1,2], both low molecular weight and polymer LCs. In monomer liquid crystals [3–11], information regarding rotations of the mesogen around the short or long axis may be obtained and the effect of the order parameter on relaxation times may be observed. In polymeric systems [12–19], a number of relaxations have been classified as α, β, γ, δ, and so on depending on the specific part of the molecular structure that is probed. In addition, by studying the nature of the temperature dependence, the underlying mechanism for activating specific molecular relaxation processes is probed. For example, the α process in polymeric systems represents cooperative motions of the backbone and its effect is observed in BDS through motions of the dipole that is coupled to the backbone. Despite the large amount of work that has been done on polymers, there is still a paucity of literature data on BDS studies of cross-linked liquid crystalline polymer (elastomer) materials [20–31]. In this paper, we use BDS to study a monomer liquid crystal and the corresponding elastomer over a wide frequency and temperature range. We assign the relaxation processes to specific molecular motions in the two cases and examine the temperature dependence to estimate the energy required for their activation. We compare these values with literature data for similar relaxation processes. The functional dependence of the relaxation rates on temperature for the monomer and polymer is studied. We show that a monomer can exhibit Vogel-Fulcher dependence of the relaxation rate on temperature.

II. EXPERIMENT

The chemical structure of the monomer (MOAC-4) is shown in Fig. 1. Differential scanning calorimetry (DSC) was performed to obtain the transition temperatures. For the monomer, nematic-isotropic (NI) transition is at 364.45 K and the crystalline-nematic transition at 345.15 K as observed by DSC at a cooling rate of 2 °C/min.

For the cross-linked polymer (CPMOAC-4), the glass transition at inflection was determined to be 318.75 K. The NI onset temperature on heating was 394.25 K with ΔH of 3.35 J/g. On cooling the IN onset was 394.05 K with ΔH of −3.49 J/g. The scanning rate was 10 °C/min. The sample was first heated to the isotropic phase at 413.15 K and then quenched to −213.15 K for 5 min before heating and cooling the sample.
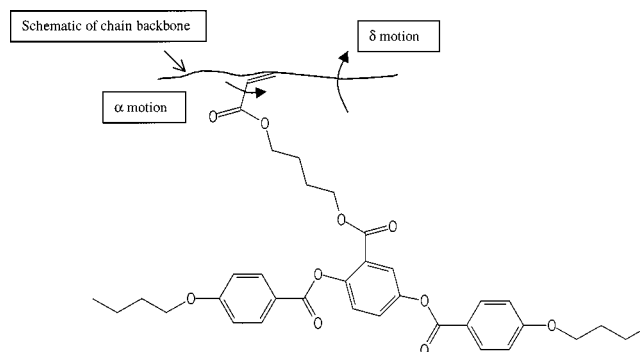
FIG. 1. Chemical structure of liquid crystal monomer. Also shown is a schematic of the monomer attachment to the backbone of the polymer chain. The curved arrows are a means to visualize the motions associated with the α and δ processes.

A. Sample preparation

For elastomer films, samples were filled in rubbed poly-(vinyl alcohol) glass cells of 50 μm thickness in vacuum at 358.15 K and reheated to 368.15 K and cooled at 1 °C/min to 348.15 K for alignment under yellow light and nitrogen. Photopolymerization was accomplished using a 75 W Oriel xenon UV lamp equipped with a 365 nm short pass, long cutoff filter with a 5 min exposure. Free standing films were obtained by removing the glass plates following heating in distilled water at 373.15 K for 20 min.

B. Experimental arrangement

Measurements of the real (ϵ') and imaginary (ϵ'') parts of the complex dielectric permittivity in the frequency range 10^{-2} Hz to 1.8 GHz were performed using a broadband dielectric spectrometer based on combination of an SI 1260, HP 4291A, Novocontrol BDC-S, and Quartro Cryosystem. For low frequency measurements from 10^{-2} Hz to 1 MHz, the SI 1260 is used in combination with the BDC-S broadband dielectric converter with the active sample cell, sample holder, sample capacitor, and active electronics that optimize the overall performance and reduce the typical noise in measurements, particularly at frequencies below 10 Hz. For the frequency range from 1 MHz to 1.8 GHz, the HP 4291A impedance analyzer based on microwave techniques was used in combination with a special rf sample cell and a precision microwave extension line connecting the sample cell to the impedance analyzer. For precise measurements of the dielectric function, the connection from the analyzer test head to the sample cell is made by a coaxial precision line with defined and nearly temperature independent propagation constants, provided by Novocontrol.

In order to keep the cable length as short as possible, the test head of the HP 4291A rf impedance analyzer is directly mounted at the top of the cryostat with the sample cell. The Quatro Cyrosystem was used for temperature control. This system allows automatic setting of the sample temperature. The main parts of the system are the cryostat, the gas jet, and the microprocessor controlled Quatro system. The Quatro consists of four independent loops controlling the sample temperature, the gas temperature (at the gas heater), the temperature of the liquid nitrogen in the Dewar, and the pressure in the Dewar. Because of the great stability of the gas pressure and the two-circuit arrangement of the gas heating, the temperature stability is better than 0.01 °C. An important characteristic of the cryosystem is the fast temperature settling time and the fact that the sample temperature approaches the set point without exceeding it. All of the system parameters are controlled by MS Windows software WINDETA provided by Novocontrol.

In the case of the monomer sample, the liquid crystal material was confined between 20 mm diameter circular gold electrode disks with 50 μm fiber optic spacers for the frequency range 1 mHz to 1 MHz. For the higher frequency range, 1 MHz to 1.8 GHz, the electrodes were 4 mm in diameter. The experiments were performed in the following manner. The samples were heated to 400 K, using ramping at the rate 1 K/min. All measurements were performed upon cooling from the initial temperature 398.1 K with temperature step of 5 K. The duration of temperature stabilization at
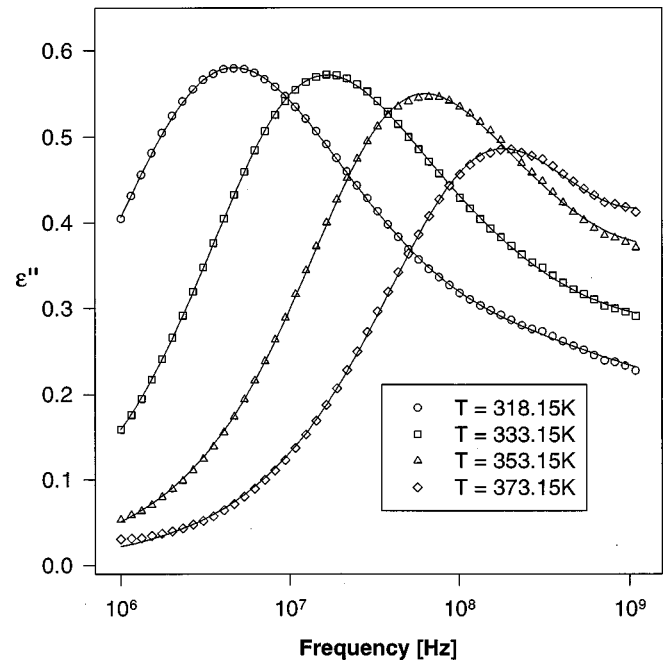
FIG. 2. Dependence of the imaginary part of the dielectric constant on frequency at four different temperatures and fits to the Havriliak-Negami function with a single relaxation term. The dielectric loss peak shifts to higher frequencies with temperature as expected.

each temperature was 20 min with an accuracy of 0.01 K. The measurements were performed at 47 and 55 different frequencies in the frequency ranges 10 mHz–1 MHz and 1 MHz–1.8 GHz, respectively.

III. RESULTS AND DISCUSSION

A. Monomer liquid crystal MOAC-4

Measurements of the imaginary part of the dielectric constant over a wide temperature range revealed a single relaxation process at high frequencies (Fig. 2). For quantitative analysis of the dielectric spectra, the Havriliak-Negami function [32,33] is used. For the case of more than one relaxation process, taking into account the contribution of the dc, conductivity to the imaginary part of the dielectric permittivity, the Havriliak-Negami function is given by

$$\varepsilon^* = \varepsilon_\infty + \sum_j \frac{\Delta\varepsilon_j}{[1+(i2\pi f\tau_j)^{1-\alpha_j}]^{\beta_j}} - i\frac{\sigma}{2\pi\varepsilon_0 f^n}, \quad (1)$$

where ε_∞ is the high frequency limit of the permittivity, $\Delta\varepsilon_j$ is the dielectric strength, τ_j is the mean relaxation time, and j numbers the relaxation process. The exponents α_j and β_j describe the symmetric and asymmetric distributions of relaxation times. The term $i\sigma/2\pi\epsilon f^n$ accounts for the contribution of conductivity, with n as fitting parameter. In the case of pure Ohmic conductivity, $n=1$. A decrease in n can be observed, as a rule, if in addition to the contribution to ε'' from the conductivity there is some influence of electrode polarization.

The parameters of the fit using the Havriliak-Negami function are shown in Table I. The dielectric strength varies from 2.43 at 308.15 K to 1.22 at 398.15 K. The α parameter

TABLE I. Parameters of the relaxation process for the monomer liquid crystal.

T (K)	τ (s)	$\Delta\varepsilon$	α	β
308.15	1.13×10^{-7}	2.43	0.408	0.854
313.15	5.86×10^{-8}	2.26	0.267	0.570
318.15	3.52×10^{-8}	2.14	0.236	0.570
323.15	2.29×10^{-8}	2.00	0.204	0.566
328.15	1.53×10^{-8}	1.99	0.165	0.494
333.15	1.03×10^{-8}	2.02	0.141	0.445
338.15	7.09×10^{-9}	2.06	0.129	0.414
343.15	5.06×10^{-9}	1.99	0.129	0.426
348.15	3.65×10^{-9}	1.93	0.129	0.426
353.15	2.81×10^{-9}	1.79	0.138	0.486
358.15	2.11×10^{-9}	1.76	0.154	0.509
363.15	1.69×10^{-9}	1.45	0.178	0.614
368.15	1.37×10^{-9}	1.34	0.179	0.688
373.15	1.08×10^{-9}	1.32	0.185	0.740
378.15	9.11×10^{-10}	1.21	0.181	0.831
383.15	7.38×10^{-10}	1.24	0.178	0.822
388.15	6.00×10^{-10}	1.22	0.178	0.822
393.15	4.89×10^{-10}	1.22	0.178	0.822
398.15	4.43×10^{-10}	1.22	0.178	0.822

which specifies the width of the relaxation is nonzero and varies from about 0.4 at the low end of the temperature range to 0.2 at the highest temperature. This indicates that the process observed has a narrow distribution of relaxation times. The asymmetry parameter β would be 1.0 for a perfectly symmetric relaxation curve. This parameter is observed to be close to 0.9 at the low end of the temperature range, goes down to about 0.43 at around 343.15 K, and then increases again to 0.8 at higher temperatures. This is evidence that the relaxation curve exhibits large deviations from symmetrical behavior close to the range where the sample becomes nematic.

Figure 3 presents the temperature dependence of the relaxation time for the monomer sample. Note that the relaxation times do not show a discontinuity at the NI transition. This is evidence of the fact that we are observing relaxations due to rotations around the long axis as these are almost unaffected by the nematic potential. The temperature dependence of this relaxation time is of non-Arrhenius type [Fig. 3(a)] and data analysis shows that it obeys the Vogel-Fulcher law [34,35] as illustrated in Fig. 3(b). The Vogel-Fulcher function is represented as

$$\tau(T)=\tau_0\exp\left(\frac{B}{T-T_0}\right), \qquad (2)$$

where τ_0 is the relaxation time at infinite temperature, B a constant related to the activation energy of the relaxation process, and T_0 the Vogel-Fulcher temperature.

The parameters describing this dependence are presented in Table II. If we determine the glass transition temperature T_g as the temperature at which $\tau_0=100\,\text{s}$ in the Vogel-Fulcher equation [36], then we obtain $T_g=256\,\text{K}$. The implication of the Vogle-Fulcher equation is that the relaxation
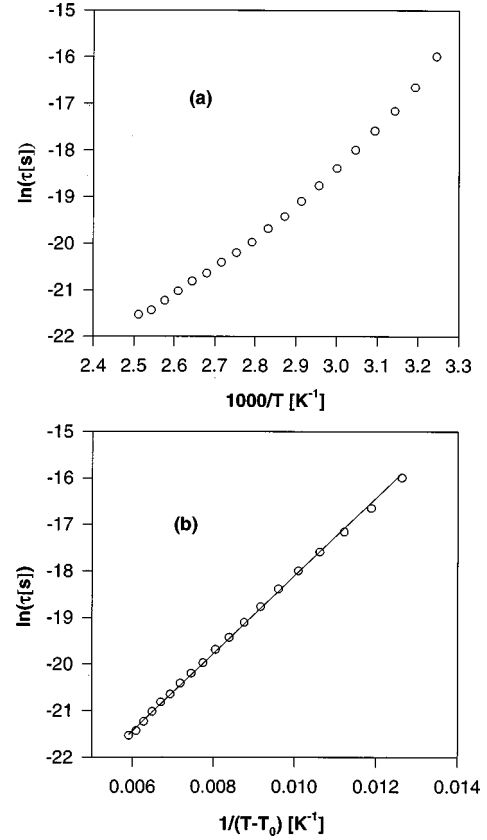
FIG. 3. (a) Plot of $\ln\tau$ vs $1000/T$ showing non-Arrhenius dependence. The relaxation times at each temperature are included in Table I. (b) Vogel-Fulcher dependence of relaxation rates is seen from plot of $\ln\tau$ vs $1/(T-T_0)$. The good agreement with the Vogel-Fulcher function is confirmed by the straight line fit.

is not an activated process although an apparent activation energy may be extracted from this equation.

There are several models that have been proposed to understand the physical meaning of this temperature dependence. The free volume approach of Grest and Cohen [37] is based on the assumption that the fractional free volume becomes zero at T_0. In a similar treatment by Donth [38,39], the volume of the cooperatively rearranging region, defined as the smallest volume element that can relax to a new configuration independently, diverges at this temperature. The good fit to this function is evidence that with this specific monomer Vogel-Fulcher behavior is indeed observed. The implications of this are not obvious since the monomer does not exhibit a glass transition temperature. It is conceivable that the side-on attachment to the mesogen perhaps gives the monomer additional free volume and that this may be responsible for the observed dependence of the relaxation rates.

TABLE II. Fitting parameters in Vogel-Fulcher equation and glass transition temperatures for monomer and polymer.

Material	τ_0 (s)	B (K)	T_0 (K)	T_g (K)
Monomer	3.1×10^{-12}	836	229	256
Polymer, process 1	9.2×10^{-7}	1050	259	316
Polymer, process 2	1.9×10^{-10}	678	285	310
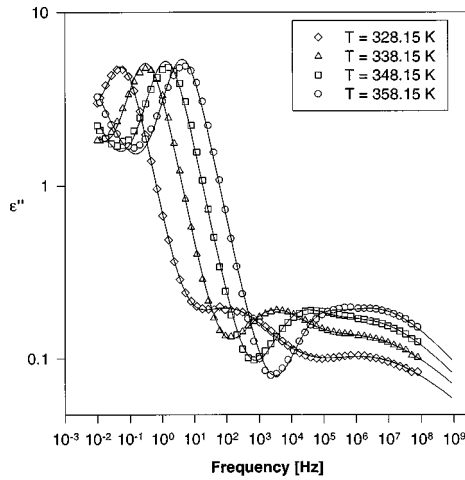
FIG. 4. Dependence of imaginary part of dielectric constant on frequency for the elastomer over the temperature range 328.15–358.15 K. The three relaxation processes are discernible in the data corresponding to 328.15 K. However, only two relaxation processes could be quantitatively analyzed.

TABLE III. Parameters of the first relaxation process (identified with the δ process) in the elastomer.

T (K)	τ_1 (s)	$\Delta\varepsilon$	α	β
323.15	9.74	10.50	0.06	1.00
328.15	2.91	9.88	0.05	1.00
333.15	1.18	10.59	0.07	1.00
338.15	5.10×10^{-1}	10.84	0.07	1.00
343.15	2.39×10^{-1}	10.95	0.07	1.00
348.15	1.21×10^{-1}	11.03	0.06	1.00
353.15	6.54×10^{-2}	11.14	0.06	1.00
358.15	3.73×10^{-2}	11.25	0.06	1.00
363.15	2.24×10^{-2}	11.40	0.06	1.00
368.15	1.41×10^{-2}	11.55	0.06	1.00
373.15	9.11×10^{-3}	11.69	0.06	1.00
378.15	6.11×10^{-3}	11.90	0.06	1.00
383.15	4.24×10^{-3}	12.19	0.06	1.00
388.15	3.02×10^{-3}	12.56	0.07	1.00
393.15	2.21×10^{-3}	13.17	0.07	1.00
398.15	1.66×10^{-3}	14.01	0.07	1.00

In order to compare activation energies for this process to literature data, we chose three temperature intervals over which the relaxation rates are approximately linear in $1/T$. The activation energy calculated using the Arrhenius function yields values of 47 kJ/mol (308.15–328.15 K), 66 kJ/mol (333.15–358.15 K), and 104 kJ/mol (363.15–398.15 K). These energies then represent the barriers to rotation of the mesogen around the long axis. Earlier literature seems to suggest that the activation energy measured in the nematic phase is indeed in the same range [8].

B. Cross-linked polymer CPMOAC-4

The imaginary part of the dielectric function as a function of frequency and temperature was measured on the polymer sample. Figure 4 shows ε'' vs f over the temperature range 328.15–358.15 K. The difference between the dielectric behavior of monomer and polymer can be seen by comparing Figs. 2 and 4. Whereas a single relaxation is observed in the case of the monomer, at least three relaxation processes can be identified in the spectra presented in Fig. 4. These processes are in the following frequency ranges: a low frequency clear relaxation process (process 1) in the frequency range 0.1–100 Hz, a second process at intermediate frequencies (100 Hz–100 kHz) (process 2), and the last one (process 3) with the smallest dielectric strength in the frequency range $f>1$ MHz. The rise of ε'' observed for temperatures $T>345$ K at frequencies $f<0.1$ Hz is due to conductivity and it is perfectly described by the third term in formula (1).

We suggest that process 1 is the δ processes. Process 2 is assigned to the α process. Process 3 could be the β process. However, process 3 is masked by the first two processes with much greater amplitude and quantitative analysis of this process is very difficult.

The δ process is well separated from the α process. However, the β process (above 1 MHz) is separated from the α process up to the temperature 353.15 K. We were able to extract relaxation times of the α process up to this temperature. Above this temperature, the peak from this process

could not be extracted due to the overlap with the β relaxation process. The α process arises due to motion of the chain backbone which manifests itself through reorientations of the ester linking the backbone to the mesogen [12]. This collective process is also called the dynamic glass transition process in the literature.

The δ process corresponds to 180° flips of the mesogen around the backbone [12]. Table III shows the dielectric parameters of this process. The dielectric strength varies from about 11 to 14 in the temperature range from 323.15 to 398.15 K. It is interesting to note that the α parameter in this case is close to zero, implying that there is hardly any distribution of relaxation times. Also, the β parameter is 1.0 at all temperatures, indicating no asymmetry at all in the dielectric loss peak. This process is clearly Debye-like in its relaxation behavior.

For the α process, whose peak values were extracted up to a temperature of 358 K, the dielectric strength is much smaller (Table IV) and varies from about 1 to 2 over the temperature range studied. Unlike the δ process, the α process shows a distribution of relaxation times as indicated by the α parameter. This is expected in a glass transition process [38]. Also, the shape of the dielectric loss peak is asymmetri-

TABLE IV. Parameters of the second relaxation process (identified with the α process) in the elastomer.

T (K)	τ_2 (s)	$\Delta\varepsilon$	α	β
318.15	1.49×10^{-1}	0.81	0.53	0.60
323.15	9.09×10^{-3}	0.96	0.5	0.62
328.15	1.38×10^{-3}	0.99	0.47	0.60
333.15	2.41×10^{-4}	0.92	0.41	0.51
338.15	6.33×10^{-5}	0.73	0.38	0.60
343.15	2.11×10^{-5}	0.62	0.33	0.60
348.15	8.17×10^{-6}	0.56	0.30	0.60
353.15	3.98×10^{-6}	0.49	0.26	0.60
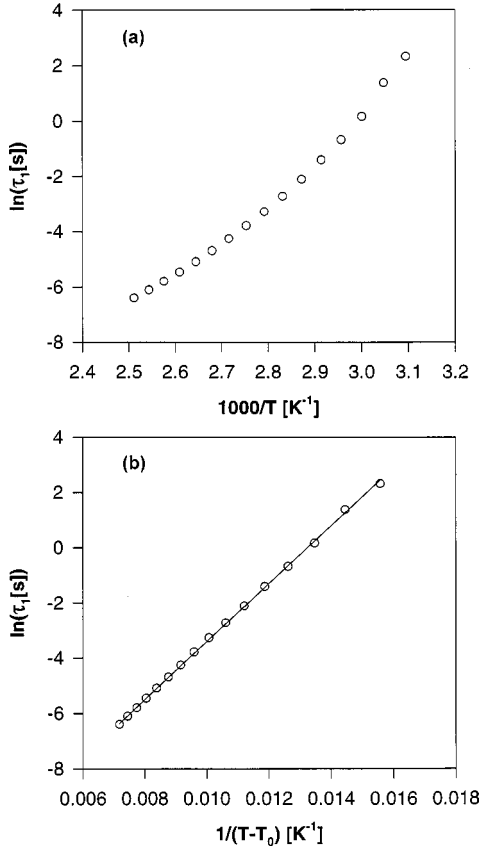
FIG. 5. (a) Plot of $\ln \tau$ vs $1000/T$ for the δ process. Parameters of this process are shown in Table III. (b) Plot showing the Vogel-Fulcher dependence of $\ln \tau_1$ vs $1/T - T_0$. As with the monomer, the good fit to the Vogel-Fulcher function is clearly seen from the fit to the data points.

cal. This asymmetry increases to a maximum of 0.2 at 363.15 K.

The temperature dependence of the relaxation rates of both α and δ processes follows a Vogel-Fulcher behavior. Figure 5(a) shows the temperature dependence plotted as $\ln \tau_1$ vs $1/T$ and Fig. 5(b) shows the dependence of the relaxation rates, illustrating the excellent fit to a Vogel-Fulcher function. Figures 6(a) and 6(b) show the dependence of the relaxation rates on temperature for the α process. Table II shows parameters of the Vogel-Fulcher fit function for the elastomer. Again, if we determine the glass transition temperature T_g as the temperature at which $\tau_0 = 100$ s [36] then we obtain $T_g = 316$ K for the δ process and 310 K for the α process.

As with the monomer, we divided the temperature regions so as to obtain an estimate of the activation energies of these processes for comparison with literature data. For the δ process, the activation energies are calculated to be 81 kJ/mol (323.15–343.15 K), 108 kJ/mol (348.15–368.15 K), and 183 kJ/mol (373.15–398.15 K). These are comparable with literature values for the δ process [41]. The temperature range for the α process is divided into two regions. The activation energies in this case are 184 kJ/mol (318.15–333.15 K) and 373 kJ/mol (338.15–353.15 K). The much higher activation, typical of α processes, indicates that the barriers to main chain motion are considerably higher in this system. The α
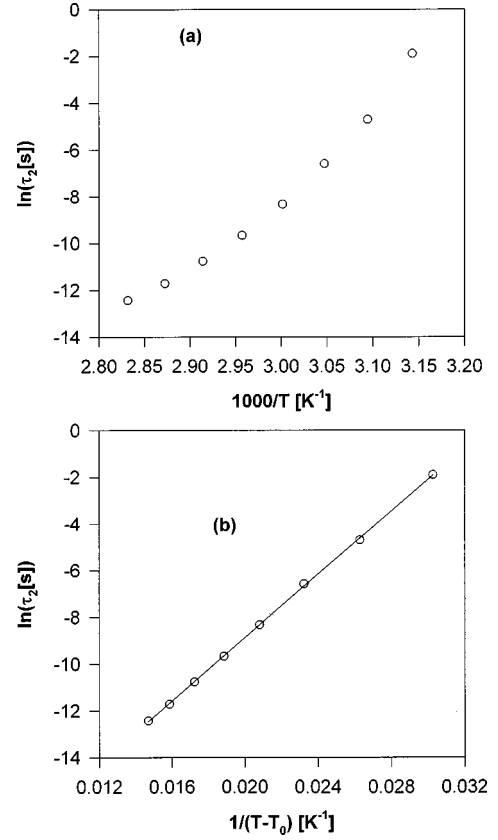
FIG. 6. (a) Temperature dependence of the relaxation rates for the α process showing non-Arrhenius dependence. (b) Plot showing Vogel-Fulcher dependence of $\ln \tau_2$ vs $1/T - T_0$.

process activation energies are typically between 150 and 350 kJ/mol according to the literature [40].

IV. CONCLUSIONS

Broadband dielectric spectroscopy is used to study relaxation processes in a nematic monomer and elastomer. In the planar geometry used in these experiments, a single relaxation is observed in the monomer whereas three relaxation processes are observed in the elastomer. Of these, we have obtained relaxation rates for two. The relaxation processes follow a Vogel-Fulcher law in both monomer and elastomer. Activation energies are calculated assuming linear approximations in restricted temperature intervals and compared with the literature, and the processes are identified with molecular relaxations in the system.

[1] *Dielectric Spectroscopy of Polymeric Materials, Fundamentals and Applications*, edited by J. P. Runt and J. F. Fitzgerald (ACS, Washington DC, 1997).

[2] Proc. SPIE **3181**, 123 (1996).

[3] H. Baessler, R. B. Beard, and M. M. Labes, J. Chem. Phys. **52**, 2292 (1970).

[4] D. Lippens, J. P. Pamieux, and A. Chapton, J. Phys. (France) **38**, 1465 (1977).

[5] J. M. Wacrenier, C. Druon, and D. Lippens, Mol. Phys. **43**, 97 (1981).

[6] J. Jadzyn, C. Legrand, P. Kedziora, and D. Bauman, J. Mol. Struct. **412**, 213 (1997).

[7] T. K. Bose, B. Campbell, S. Yagihara, and J. Thoen, Phys. Rev. A **36**, 5767 (1987).

[8] H. G. Kruel, S. Urban, and Wurflinger, Phys. Rev. A **45**, 8624 (1992).

[9] G. R. Luckhurst and R. N. Yeates, Chem. Phys. Lett. **38**, 551 (1976).

[10] G. P. Sinha and F. M. Aliev, Phys. Rev. E **58**, 2001 (1998).

[11] W. H. de Jeu, C. J. Gerritsma, P. Van Zanten, and W. J. A. Goossens, Phys. Lett. **39A**, 355 (1972).

[12] R. Zentel, G. R. Strobl, and H. Ringsdorf, Macromolecules **18**, 960 (1985).

[13] U. F. Gedde, D. Buerger, and R. H. Boyd, Macromolecules **20**, 988 (1987).

[14] H. Kresse, S. Kostromin, and V. P. Shibaev, Makromol. Chem., Rapid Commun. **3**, 509 (1982).

[15] H. Kresse and V. P. Shibaev, Makromol. Chem., Rapid Commun. **5**, 63 (1984).

[16] W. Heinrich and B. Stoll, Colloid Polym. Sci. **263**, 895 (1985).

[17] F. J. Bormuth and W. Haase, Liq. Cryst. **3**, 881 (1988).

[18] K. L. Ngai, A. Schonlas, and E. Schlosser, Macromolecules **25**, 4915 (1992).

[19] F. Kremer, S. U. Vallerien, R. Zentel, and H. Kapitza, Macromolecules **22**, 4040 (1989).

[20] R. Sigel, W. Stille, G. Strobl, and R. Lehnert, Macromolecules **26**, 4226 (1993).

[21] H. R. Brand and H. Finkelman, in *Handbook of Liquid Crystals*, Vol. 3, edited by D. Demus, J. Goodby, G. W. Gray, H.-W. Spiess, and V. Vill (Wiley-VCH, New York, 1998), Chap. 5.

[22] T. Pakula and R. Zentel, Makromol. Chem. **192**, 2401 (1991).

[23] K. H. Hanus, W. Pechold, F. Soergel, B. Stoll, and R. Zentel, Colloid Polym. Sci. **268**, 222 (1990).

[24] J. Kupfer and F. Finkelman, Makromol. Chem., Rapid Commun. **12**, 717 (1991).

[25] W. Kaufhold and H. Finkelman, Makromol. Chem. **192**, 2555 (1991).

[26] M. Warner and E. M. Terentjev, Prog. Polym. Sci. **21**, 853 (1996).

[27] E. M. Terentjev, J. Phys.: Condens. Matter **11**, R239 (1999).

[28] M. Hebert, R. Kant, and P. G. de Gennes, J. Phys. I **7**, 909 (1997).

[29] F. J. Davis and G. R. Mitchell, Polymer **37**, 1345 (1996).

[30] P. M. S. Roberts, G. R. Mitchell, and F. J. Davis, J. Phys. II **7**, 1337 (1997).

[31] A. J. Symons, F. J. Davis, and G. R. Mitchell, Polymer **40**, 5365 (1999).

[32] S. Havriliak, Jr. and S. J. Negami, Polym. Sci. Ser. C **14**, 99 (1966).

[33] S. Havriliak, Jr. and S. Negami, Polymer **8**, 161 (1967).

[34] H. Vogel, Phys. Z. **22**, 645 (1921).

[35] G. S. Fulcher, J. Am. Chem. Soc. **8**, 339 (1925).

[36] *Disorder Effects on Relaxational Processes*, edited by R. Richert and A. Blumen (Springer-Verlag, Berlin, 1994).

[37] G. S. Grest and M. H. Cohen, Adv. Chem. Phys. **48**, 455 (1991).

[38] E. Donth, *Relaxation and Thermodynamics in Polymers: Glass Transition* (Akademie-Verlag, Berlin, 1992).

[39] A. Schonhals, in *Dielectric Spectroscopy of Polymeric Materials, Fundamentals and Applications* (Ref. [1]).

[40] G. P. Simon, in *Dielectric Spectroscopy of Polymeric Materials, Fundamentals and Applications* (Ref. [1]).

[41] T. Yu, K. Devanand, A. M. Jamieson, and R. Simha, Polymer **32**, 1928 (1991).